Physiological role for amyloid precursor protein in adult experience-dependent plasticity

Sally A. Marik[a], Olav Olsen[b], Marc Tessier-Lavigne[a], and Charles D. Gilbert[a,1]

[a]Laboratory of Neurobiology, The Rockefeller University, New York, NY 10065; and [b]Laboratory of Brain Development and Repair, The Rockefeller University, New York, NY 10065

Contributed by Charles D. Gilbert, May 27, 2016 (sent for review March 16, 2016; reviewed by Ulf T. Eysel and Jon H. Kaas)

Changes in neural circuits after experience-dependent plasticity are brought about by the formation of new circuits via axonal growth and pruning. Here, using a combination of electrophysiology, adeno-associated virus–delivered fluorescent proteins, analysis of mutant mice, and two-photon microscopy, we follow long-range horizontally projecting axons in primary somatosensory cortex before and after selective whisker plucking. Whisker plucking induces axonal growth and pruning of horizontal projecting axons from neurons located in the surrounding intact whisker representations. We report that amyloid precursor protein is crucial for axonal pruning and contributes in a cell autonomous way.

axon pruning | long-range axons | amyloid precursor protein | somatosensory cortex | experience-dependent plasticity

Alterations in sensory experience lead to substantial modifications in cortical circuits. This plasticity is mediated, in part, through changes in the strength of synaptic transmission, but can also involve massive anatomical changes that include the sprouting of new axon collaterals, pruning of existing collaterals (1–3), and turnover of synapses along stable axons. After sensory loss, the cortical topography of the sensory map is permanently altered within the lesion projection zone (LPZ), the area of the cortex that receives input from the deafferented part of the periphery (4). Initially, the LPZ is silenced, but it subsequently recovers sensory input by the sprouting of afferents originating from nondeprived regions of the sensory periphery. This culminates in the reorganization of the cortical topographic map (4, 5). We have previously demonstrated that this reorganization of the cortical map is mediated through anatomical changes in horizontally projecting axons of layer II/III neurons within and around the LPZ (1–3). Electrophysiological changes occur along the same temporal scale (4, 5).

Axonal changes associated with adult cortical plasticity are seen for both excitatory neurons, which send enriched projections into the LPZ, and inhibitory neurons located within the LPZ, which send reciprocal connections outside the LPZ (1–3). Previously, we demonstrated that axonal pruning after sensory deprivation (e.g., selective whisker plucking) requires death receptor 6 (DR6) (6). DR6 interacts with the E2 domain of amyloid precursor protein (APP) (7, 8), and together, these proteins initiate an apoptotic cascade that mediates axon pruning in the absence of cell body death during development (8–10). It remains to be determined whether DR6-mediated pruning of axons after sensory deprivation in the adult may also involve APP.

APP is best known for its role in Alzheimer's disease, where proteolytic cleavage of APP by beta- and gamma-secretases liberates Aβ (11), which impairs synaptic plasticity (12) and is thought to induce neuronal cell death. However, the physiological roles for APP are slowly coming into focus. Under normal conditions, APP is present on both sides of the synapse (13–18). $APP^{-/-}$ mice show performance deficits in cognitive tasks (19), as well as defects in social learning (20–22). These deficits may be attributed to the reduced number of dendritic spines, shorter dendritic length, and smaller brains observed in these mutant mice (23–26). It remains to be determined how APP functions in these processes, but recent work has demonstrated that the E1 portion of APP mediates cellular adhesion (27), whereas the E2 domain is involved in developmental axonal pruning (8). Here, we demonstrate that APP also plays an integral role in axonal pruning in response to experience-dependent plasticity in the adult.

Results

To investigate a role for APP in axonal pruning, electrophysiological recordings in the somatosensory cortex of mice were used to locate the C3 barrel for the injection of genetically engineered viruses to label cortical neurons. After complete expression of the adeno-associated virus (AAV) proteins, axons were imaged using a two-photon microscope. This allowed us to follow the structural plasticity of axons projecting into the lesion projection zone (LPZ) in vivo and determine axonal growth and pruning after sensory loss. Axonal dynamics of $APP^{-/-}$ and $APP^{flox/flox}$ mice compared with littermate controls after whisker plucking were examined.

We focused our study on the axons of C row-labeled neurons that project into D and E rows for $APP^{-/-}$ and *WT* animals. One day after the removal of whisker rows D and E, we observed comparable axonal growth between $APP^{-/-}$ and *WT* animals ($APP^{-/-}$ = 27.04 ± 2.8%; *WT* = 56.3 ± 29.2%; $P = 0.44$). However, during this same period, axonal pruning was almost completely blocked in $APP^{-/-}$ animals compared with in *WT* animals (0.26 ± 0.26% and 77.5 ± 1.3%, respectively; $P < 0.001$; Figs. 1 and 2). After 2 d of plucking, only 0.39% (±0.4%) of axons in $APP^{-/-}$ animals were pruned, whereas 67.8% (±8.4%) of the initial axons present during baseline in *WT* animals were pruned ($P < 0.001$ level). As for the growth of new axons after 2 d of plucking, the length of axon collaterals in $APP^{-/-}$ mice increased by 283.2% (±110.1%) with respect to baseline, whereas axonal length in *WT* animals increased by 38.9% (±10.7%) and was significantly different ($P = 0.04$). After 7 d of plucking, $APP^{-/-}$ mice still showed no signs of axon pruning with respect to baseline (0.6 ± 0.06%), which was significantly different compared with *WT* animals (−76.8 ± 9.7%; $P = 0.001$; Fig. 2).

Significance

Amyloid precursor protein (APP) has long been implicated in Alzheimer's disease, but its normal physiological role has only recently come to light. Here we demonstrate that APP plays a key role in axonal pruning after experience-dependent plasticity in the adult. Furthermore, we show that APP operates in a cell-autonomous fashion in the cortex to induce axonal pruning after sensory loss. APP is therefore important for the normal process of adult cortical plasticity through its role in the sculpting of axonal arbors.

Author contributions: S.A.M., O.O., M.T.-L., and C.D.G. designed research; S.A.M. and C.D.G. performed research; M.T.-L. contributed new reagents/analytic tools; S.A.M., O.O., M.T.-L., and C.D.G. analyzed data; and S.A.M., O.O., M.T.-L., and C.D.G. wrote the paper.

Reviewers: U.T.E., Ruhr-Universität Bochum; and J.H.K., Vanderbilt University.

The authors declare no conflict of interest.

[1]To whom correspondence should be addressed. Email: gilbert@rockefeller.edu.

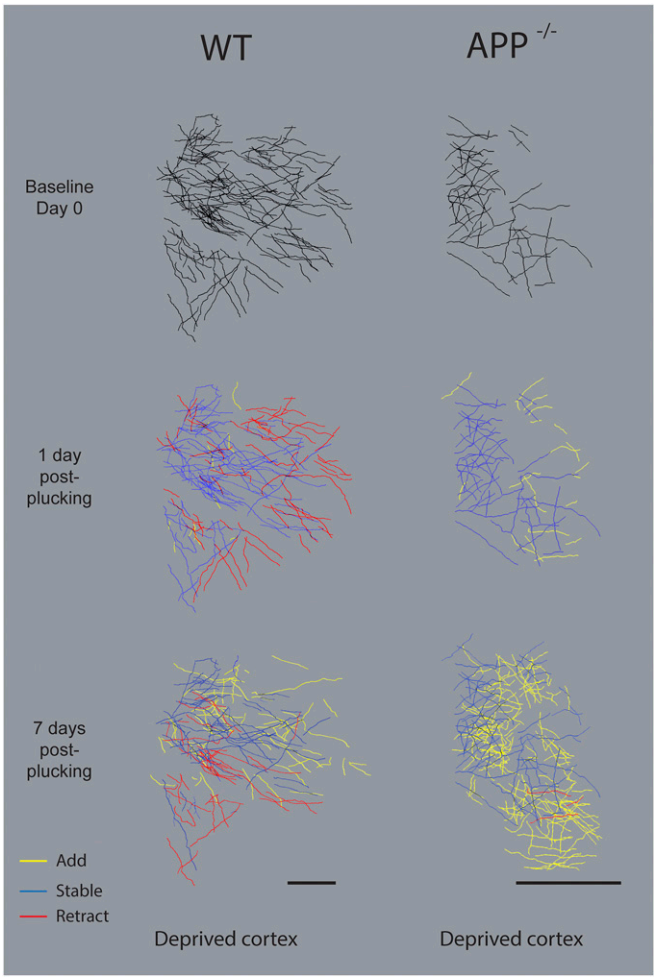

Fig. 1. Axonal pruning that accompanies experience-dependent plasticity is regulated by APP. Reconstructions of horizontally projecting axonal arbors present in deprived whisker rows D and E in two exemplar mice: one *APP*$^{-/-}$ (*Right*) and one *WT* littermate (*Left*). AAV injection was located in C3, which labeled C3 layer II/III neurons and their axons. Shown is the reconstruction of axons present in rows D and E, which will become the LPZ. Black represents the initial image to which images from later times are compared. Subsequent reconstructions are color coded to represent stable axons as blue, retracted axons as red, and added axons as yellow compared with previous times. (Scale bar, 200 μm.)

Axonal growth for *APP*$^{-/-}$ mice (388.3 ± 57%) was not significantly different ($P = 0.61$ *t* test) than for *WT* mice (187.1 ± 135.7%) 7 d after whisker plucking. In summary, axons of *APP*$^{-/-}$ mice underwent significantly less pruning compared with *WT* animals at all times after whisker plucking.

To overcome complications associated with constitutive deletion of *APP* and to assess cell autonomy, we examined axon plasticity after selective whisker deprivation, using *APP*$^{flox/flox}$ mice to knock out APP expression in the adult just before whisker plucking. To identify APP-deficient neurons, a combination of two AAVs (1:1) were injected: one encoding Cre-GFP and a second encoding floxed tdTomato to confirm cre-expression. Both constructs used the human synapsin promoter, and doubly labeled neurons were subject to analysis. Test injections confirmed that every tdTomato-expressing neuron also expressed Cre-GFP in its nucleus (Fig. 3*B*). We examined five injections in three animals and found 97.8% colocalization, whereas only 2.2% of neurons expressed Cre only. Axons of *APP*$^{flox/flox}$ animals were imaged at baseline and 2 d after plucking. As observed in *APP* null animals, axonal pruning was significantly impaired in APP-deficient neurons, with only 0.07 ± 0.07% of axons being pruned at 2 d after whisker plucking compared with 49.5 ± 3.9% of axons in control ($P < 0.01$, *t* test). In contrast, axonal growth between APP-deficient and control neurons was not significantly different at 2 d, adding 495.7 ± 200% and 176.6 ± 71.9% of axonal arbors ($P = 0.25$), respectively. These results are consistent with those observed for the APP null and indicate that APP acts cell autonomously to mediate axonal pruning after whisker deprivation in the adult (Fig. 3*A*).

Previous studies report that *APP*$^{-/-}$ mice have a reduced dendritic length compared with *WT* littermates (26). However, it is not clear whether the axonal arbors of neurons in *APP*$^{-/-}$ mice would also be reduced compared with their littermate controls. Previously, we reported that axons in *DR6* mutant mice were significantly longer than their *WT* littermates, suggesting impaired axonal pruning during development. Because DR6 interacts with APP and both mouse mutants show similar phenotypes in axonal plasticity after whisker deprivation, we examined whether axonal length was also different in *APP*$^{-/-}$ mice compared with littermate controls. The radius of axonal range from the injection site was determined by measuring the center of the injection site to the tip of the furthest reaching arbor during baseline imaging sessions for *WT*, *APP*$^{-/-}$, and *DR6*$^{-/-}$ (previously studied) animals. We found that the axonal arbor range in *APP*$^{-/-}$ mice (658.7 ± 55.7 μm) did not differ significantly from the horizontal projection range in *WT* mice (709.9 ± 64.5 μm; $P = 0.40$; Fig. 4*A*). *DR6*$^{-/-}$ mice (909.7 μm ±133.7), in contrast, had significantly longer axons at baseline compared with *APP*$^{-/-}$ and *WT* mice (Fig. 4*A*; $P = 0.05$, *t* test).

Overall axonal structure in *APP* mutants differed only slightly from that in *WT* animals. We did not observe abnormal reversals of axon trajectory in *APP*$^{-/-}$ or *APP*$^{flox/flox}$ mice, which had been previously seen in *DR6*$^{-/-}$ animals (6). However, the number of axon branch points was significantly increased in *APP*$^{-/-}$ mice compared with *WT* littermates. Furthermore, the number of secondary axons diverging from the primary axon at 90 degree angles or greater were significantly increased in *APP*$^{-/-}$ mice (Fig. 2*B*) compared with *WT* or *DR6*$^{-/-}$ animals, as were the number of branch points at 90 degrees or more. Under baseline conditions, these 90 degree bifurcations were present at 1.14 ± 0.29 occurrences/mm examined in *APP*$^{-/-}$ animals compared with 0.26 ± 0.0001 occurrences/mm in *WT* animals (Fig. 2*C*). Branch points that were less than 90 degrees were also elevated in basal conditions, at 0.98 ± 0.27 occurrences/mm in *APP*$^{-/-}$ compared with 0.53 ± 0.09 occurrences/mm in *WT* animals (Fig. 2*D*). Two days after whisker plucking, the number of 90 degree or greater bifurcations was still elevated for *APP*$^{-/-}$ mice (1.79 ± 0.23) compared with *WT* mice (1.14 ± 0.33; Fig. 2*C*), whereas the observed rate at 2 d for axonal branchings that were less than 90 degrees was higher for *WT* (2.99 ± 1.29) than *APP*$^{-/-}$ (0.81 ± 0.27; Fig. 2*D*) mice. We also examined branch points in *APP*$^{flox/flox}$ mice and observed an occurrence of branch points equal to or greater than 90 degrees at an occurrence rate of 0.09 ± 0.20 during baseline and 0.52 ± 0.33 after 2 d of plucking (Fig. 2 *C* and *D*). Branch points that were at an angle less than 90 degrees occurred at a rate of 0.56 ± 0.03 during baseline and 0.47 ± 0.22 after 2 d of whisker plucking (Fig. 2*D*).

To determine the effect of *APP*$^{-/-}$ on synaptic load, we analyzed bouton density on stable axons (axons that did not prune or grow). During baseline, bouton density for stable axons did not significantly differ between *WT* (0.032 ± 0.005 boutons/μm) and *APP*$^{-/-}$ (0.042 ± 0.005 bouton/μm) mice ($P = 0.29$; Fig. 4*B*). However, 1 d after whisker plucking, *APP*$^{-/-}$ mice had a significant increase in the number of boutons present (0.060 ± 0.005 bouton/μm) compared with *WT* animals (0.027 ± 0.004 boutons/μm; $P = 0.0005$, *t* test). Thus, rather than compensating for the lack of axonal pruning by decreasing bouton density, the reverse occurred. After 2 d of

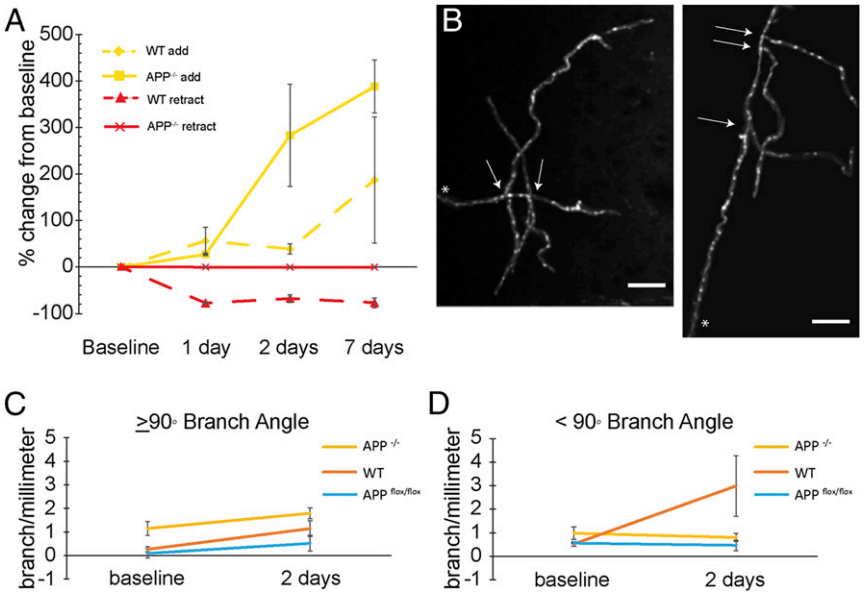

Fig. 2. Quantification of axonal arbors in $APP^{-/-}$ mice compared with *WT* mice. (*A*) Mean percentage change for axonal growth and axonal pruning are plotted with error bars representing ±SEM. Axonal growth is represented as positive numbers, and axonal pruning as negative numbers. Solid yellow represents percentage change in axonal growth in $APP^{-/-}$ mice, and dashed yellow represents axonal growth in *WT* animals. Axonal pruning is plotted on the negative axis: the solid red line represents axonal pruning in $APP^{-/-}$, and the dashed red line represents axonal pruning in *WT* mice. (*B*) Examples of axonal arbors in $APP^{-/-}$ mice after whisker plucking. Arrows depict abnormal axonal morphology of axonal branches that occur at 90 degrees or more. In both examples, the cell body is located to the left of the image and denoted with an asterisk. (Scale bar, 30 μm.) (*C*) Quantification of the number of secondary axons diverging from the primary axon at a 90 degree angle or greater. $APP^{-/-}$, yellow; *WT*, orange; and $APP^{flox/flox}$, blue. (*D*) Quantification of the number of secondary axons diverging from the primary axon at less than 90 degrees. $APP^{-/-}$, yellow; *WT*, orange; and $APP^{flox/flox}$, blue.

whisker plucking, axons that were stable during the imaging period had a density of 0.043 ± 0.010 boutons/μm for $APP^{-/-}$ mice and 0.034 ± 0.007 boutons/μm for *WT* mice. Bouton density for $DR6^{-/-}$ mice (0.075 ± 0.005 boutons/micrometer) was statistically different from $APP^{-/-}$ even at baseline ($P = 0.003$, *t* test), as well as 2 d after plucking (0.097 ± 0.009 bouton/μm; $P = 0.036$, *t* test). However, bouton density between $DR6^{-/-}$ (0.712 ± 0.007 boutons/μm) and $APP^{-/-}$ at 1 d after plucking were not significantly different ($P = 0.244$, *t* test).

We also examined bouton turnover rates on stable axons. There was no significant difference in the addition of boutons among $APP^{-/-}$, *WT,* and $DR6^{-/-}$ animals in the first 2 d of whisker plucking (Fig. 4*C*). However, $APP^{-/-}$ animals showed significantly more bouton elimination (35.8% ± 9.68) at 2 d whisker plucking compared with *WT* (12.5% ± 7.64; $P = 0.03$), but not *DR6* (23.73% ± 6.54; $P = 0.38$) mice.

We examined the bouton density on all axons; stable, retracted, and new axons through the first 2 d of whisker plucking (Fig. 4*D*). Overall bouton density was not significantly different between $APP^{-/-}$ and *WT* ($APP^{-/-}$: 0.042 ± 0.005 boutons/μm; *WT*: 0.040 ± 0.007 boutons/μm; $P = 0.8$). However, $DR6^{-/-}$ total bouton density was significantly elevated during baseline imaging sessions (0.075 ± 0.004 boutons/μm; $P = 0.001$). After 1 d of whisker plucking, total bouton density was not significantly different among *WT*, $APP^{-/-}$, or $DR6^{-/-}$ mice ($APP^{-/-}$: 0.043 ± 0.008011 boutons/μm; *WT*: 0.033 ± 0.011 boutons/μm; $DR6^{-/-}$: 0.032 ± 0.007 boutons/μm; $P = 0.61$, ANOVA). There was also no significant difference at 2 d of whisker plucking ($APP^{-/-}$: 0.045 ± 0.008; *WT*: 0.045 ± 0.02; $DR6^{-/-}$: 0.039 ± 0.008; $P = 0.95$, ANOVA).

Discussion

Our studies demonstrate that APP is crucial for axonal pruning in the adult somatosensory cortex after sensory loss. Axonal growth and pruning are important for rewiring cortical topography after sensory loss (1–3). Excitatory neurons located in the peri-LPZ undergo axonal growth and pruning in response to sensory loss (e.g., whisker plucking). Experience-dependent axonal growth and pruning occur on the same time frame as the observed topographic remapping (4, 5). Determining the underlying molecular mechanisms for this cortical rewiring is crucial for our understanding of experience-dependent plasticity and what may go awry during neurodegeneration. Here, we demonstrate that APP plays an integral role in healthy axonal pruning in the adult in response to sensory manipulation. In both the constitutive and conditional APP knockouts, axonal pruning was almost entirely blocked, leading to more dense and extensive axonal arbors. Because this effect was seen in both the conditional and constitutive knock out, APP operates in a cell autonomous way to mediate axonal pruning. Previously, we reported that DR6 is necessary for axonal pruning after sensory loss (6). DR6 has been shown to interact with APP (7, 8) to induce an apoptotic pathway (10) that initiates axonal pruning (9). Taken together, these data suggest APP and DR6 coordinate experience-dependent plasticity and axonal pruning in the adult brain.

Although overall length of axons in $APP^{-/-}$ mice was similar to that in *WT* animals, their gross overall structure differed from *WT* animals, with more branch points at baseline and a greater number of branch points that were 90 degrees or more from the primary branch. One reason that $DR6^{-/-}$ animals may have more wide-ranging axonal arbors is because of a possible role of DR6 in limiting growth, or the inability to prune during development. However, $APP^{-/-}$ mice might also be expected to experience a failure to prune during development, yet their axonal arbor length is not significantly different from that of *WT* animals. Furthermore, our study demonstrates that the DR6/APP pathway that has been demonstrated to play an important role during development (9) is conserved and plays an important role in structural plasticity of axons later in life. During development, the interaction between DR6 and APP can be prompted by the

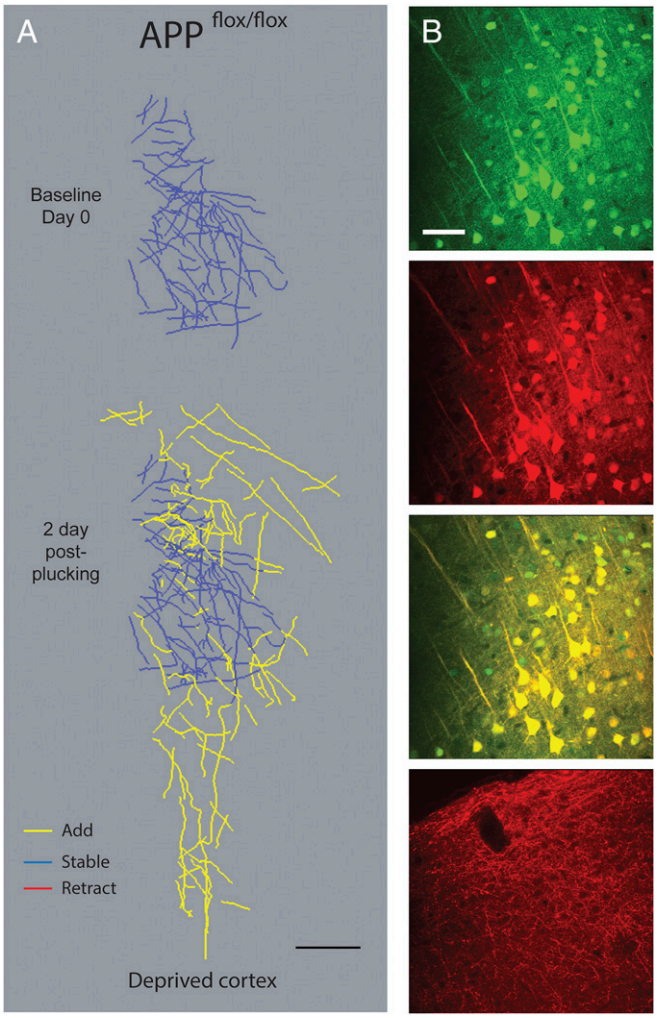

Fig. 3. Axonal pruning that accompanies experience-dependent plasticity is regulated by APP in a cell autonomous fashion. Reconstructions of horizontally projecting axonal arbors present in deprived rows D and E of an exemplar $APP^{flox/flox}$ mouse. AAV injection was located in C3, which labeled C3 layer II/III neurons and their axons. Shown is the reconstruction of axons projecting into rows D and E, which will become the LPZ. Baseline reconstruction is on top, and reconstruction at 2 d after plucking is below. Axons are color coded to represent stable axons as blue, retracted axons as red, and added axons as yellow compared with baseline. (Scale bar, 200 μm.) (*B*) Colocalization of Cre expression and tdTomato expression after coinjection of two AAVs encoding GFP-Cre and a FLEX tdTomato. (*Top*) Cre-GFP infected cells. (*Upper Middle*) tdTomato expression from FLEX tdTomato AAV infection (with Cre activation). (*Lower Middle*) Colocalization of Cre-expressing neurons and tdTomato-expressing neurons. (*Bottom*) Axons expressing tdTomato from coinfection. (Scale bar, 50 μm.)

removal of neurotrophins from the target region. It is still unknown what stimulates the DR6 and APP interaction in the adult. Although neurotrophins are expressed at very low amounts in the adult compared with the developing organism, it is possible that the DR6/APP interaction in the adult is also mediated by change in neurotrophin expression (28) that occurs in the LPZ after sensory loss (28). The details and specifics of whether and how neurotrophins initiate the DR6/APP interaction in the adult will need to be addressed in future research.

APP operates in a cell autonomous fashion to mediate axonal pruning in the adult after changes in sensory input, similar to its cell autonomous role in sensory neuron and retinal axon pruning (8, 29). Previous work demonstrates that APP is expressed both pre- and postsynaptically (13–18) and is present in growth cones (30, 31). Furthermore, the E1 portion of the APP protein plays a role in cell adhesion (27). Loss of the APP intracellular domain or last 15 amino acids results in synaptic dysfunction and impaired plasticity (32). Overexpression of APP increases the number of dendritic spines, whereas spine density is significantly lower for $APP^{-/-}$ mice (23). APP has been shown to play a role in sequestering of GluR2 at synaptic sites (23). Taken together, these suggest APP plays an important role in controlling synaptic contacts both on a morphological level and on a functional level.

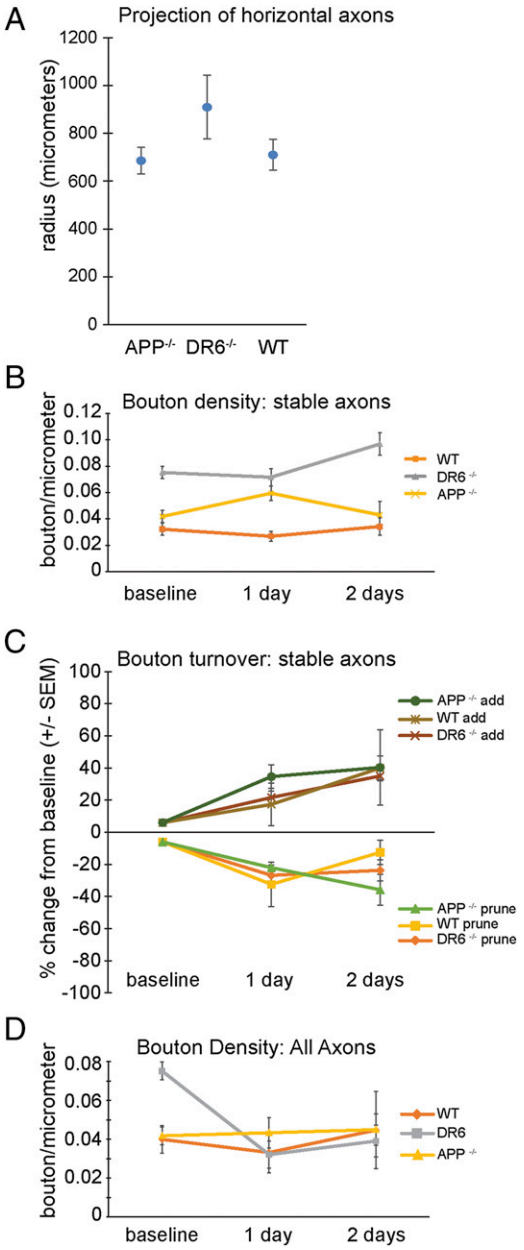

Fig. 4. Analysis of axonal arbors and boutons. (*A*) Radius of horizontal projection of axons (mean ± SEM) for $APP^{-/-}$, $DR6^{-/-}$, and *WT* animals. (*B*) Bouton density on stable axons through first 2 d of whisker plucking. *WT*, orange; $APP^{-/-}$, yellow; and $DR6^{-/-}$, gray. (*C*) Percentage bouton turnover on stable axons. Percentage change of added from baseline depicted on the positive *x* axis and percentage change pruned from baseline is depicted on the negative *x* axis. (*D*) Bouton density for all axon types (stable, added, to-be-pruned) through first 2 d of whisker plucking. *WT*, orange; $APP^{-/-}$, yellow; and $DR6^{-/-}$: gray.

We observed that bouton density on stable axons in $APP^{-/-}$ mice was no different from that in *WT* animals at the baseline time. There was a transient significant increase in the number of boutons on stable axons at 1 d after plucking compared with *WT* animals that was observed to be quickly pruned back by day 2. Between day 1 and day 2 of whisker plucking, we also observed an increase in bouton pruning on axons that did not undergo axonal growth or pruning. This suggests that although the ability to create new presynaptic contacts is not altered in $APP^{-/-}$ mice, the ability to retain these contacts may be altered, as shown by the significant pruning of boutons after 2 d of plucking (Fig. 4*C*). The bouton density of stable axons in $DR6^{-/-}$ mice was elevated at baseline and remained elevated after experience-dependent plasticity compared with in *WT* mice. We also examined the bouton density on all axons, regardless of their fate (stable, to be pruned, or newly formed). Total bouton density of $APP^{-/-}$ mice did not significantly differ compared with that of *WT* mice at baseline or the first 2 d of whisker plucking. For $DR6^{-/-}$ mice, total bouton density levels were significantly higher than *WT* at baseline imagine sessions but approached *WT* levels after experience-dependent plasticity. The difference in bouton density on stable axons and all axons reflects a decrease in the number of boutons on new axons. Furthermore, the lack of pruning in $DR6^{-/-}$ and $APP^{-/-}$ mice suggests an overall increase in synaptic density within the LPZ; therefore, APP may play a role in synaptic homeostasis. We do not know, however, whether the exuberant growth of horizontal connections after whisker plucking that is not accompanied by pruning could be compensated by reduced inputs from other classes of connections.

Here we demonstrate that APP plays a key role in axonal pruning in the adult in response to changes in experience, providing a physiological role for APP in the adult brain. Although the deleterious effects of APP mutations in Alzheimer's disease may be in part a result of its role in plaque formation and neurodegeneration, it will be of interest to determine whether they also contribute by interfering with its normal role in axonal pruning in the adult. Furthermore, our findings lend evidence to the fact that not all axonal and bouton pruning are pathological changes, but instead, are part of the normal process of local circuit dynamics in the adult brain. Our work here suggests that APP, a key protein in neurodegeneration, may play an integral part in healthy brain function that is important for cognition and adapting to the world around us. Here we have used a model of sensory deprivation as a means of altering sensory experience that leads to axonal remodeling. Going forward, it will be of value to determine whether normal perceptual learning, also known to affect function in early sensory cortex, is associated with similar axonal changes as those we see here, and whether APP plays a similar role in mediating these changes.

Materials and Methods

Adult $APP^{-/-}$ (Genentech) and conditional $APP^{flox/flox}$ mice (17) and their wild-type littermates were used. For comparison, we include previously reported data from $DR6^{-/-}$ mice (6). AAV injections were done after postnatal day 60 (P60), and the first imaging session was performed at least 3 wk later. Methods were previously described (1, 6). All procedures were performed in accordance with institutional and federal guidelines for the treatment of animals.

Virus Preparation. Excitatory neurons in $APP^{-/-}$ and *WT* animals were labeled with an AAV2/1 vector that contained the alpha-CaMKII promoter sequence and tdTomato fluorescent protein sequence, with a titer of 1×10^{12} particles/mL. Virus preparation has been described previously (1). For $APP^{flox/flox}$ animals, a combination of two AAVs, encoding GFP-Cre and a FLEX tdTomato (UPenn Vector Core), were used to label and conditionally knock out APP in the neurons labeled with the virus. This allowed us to label only one barrel whose topographic location was determined electrophysiologically, and then to express Cre to knockout *APP* and fluorescently label those neurons.

Viral Injection and Cranial Window Surgery. All procedures were followed according to institutional and federal guidelines. Methods have been described previously (1, 6). Briefly, adult mice (>P60) were anesthetized with ketamine (80 mg/kg) and xylazine (6 mg/kg); a craniotomy, with dura intact, was performed over barrel cortex; the barrel topography was mapped electrophysiologically; and an AAV was injected into the C3 barrel at a depth of 250–350 μm from cortical surface. The amount of AAV to be injected was based on viral titer and preliminary injections that determined the amount of lateral spread resulting from the injection. The craniotomy was sealed with a 3-mm circular glass coverslip secured with dental acrylic. Animals were recovered on a heating blanket and returned to their home cage for a minimum of 3 wk to ensure full expression of the virus before imaging occurred.

Imaging. Animals were anesthetized with isoflurane (3% induction, 1.5–2% maintenance), and axons projecting into deprived rows were imaged. We used 26 mice for this study, and most mice were imaged for more than one postplucking time. Images were collected on a custom-built two-photon microscope with a scanning head, which was moveable in three dimensions, using a Sutter MP-285–3Z micromanipulator. The laser source was a Ti-sapphire laser (Tsunami/Millenia System; Spectra Physics). Images were acquired with ScanImage. Images were taken of injection site and deprived rows by overlapping stacks to ensure reconstruction of axonal arbors.

After the baseline imaging session every other day, animals were anesthetized with isoflurane and whiskers from rows D and E were examined under a dissecting microscope, and if there was regrowth, the whisker was plucked. Subsequent imaging was done for variable intervals after the onset of the whisker plucking.

Analysis. Images were viewed offline with ImageJ (https://imagej.nih.gov/ij/) and deconvolved using Huygens deconvolution software (Scientific Volume Imaging). Axons were traced via the semiautomatic mode in Neuromantic (v1.6.3; www.reading.ac.uk/neuromantic/html/body_download.html), and the reconstruction's voxel size was corrected with a custom Matlab (Mathworks) program.

We reconstructed a total of 736.62 mm labeled axonal arbors from $APP^{-/-}$, $APP^{flox/flox}$, and *WT* animals for this study. Images were aligned and tiled in Neuromantic and traced while examining the images in three dimensions. After reconstruction, axons were coded as stable, pruned, or added in relation to the baseline imaging session. Axonal pruning and axonal growth were calculated by taking the axonal length of the class of axon (stable, prune, or added) for a given point and dividing it by the total length of axons present at baseline and then reported as a percentage change. Axonal branch points were observed and quantified as equal to or greater than 90 degrees from the axis of projection of the axon or less than 90 degrees. Quantification of bouton dynamics was done by noting boutons present and then comparing images of the axon at baseline and at specific times. Boutons were quantified as added, stable, or retracted. Axonal radius was quantified by measuring from the center of the injection site and the tip of the furthest reaching axon in manual mode of Neuromantic, which produces a SWC file.

Statistical Analysis. Student's *t* test was used to determine statistical significance between genotypes at the same time. F-test was used to determine whether there was a statistical significance of initial area measurements between $APP^{-/-}$ and *WT* and $APP^{flox/flox}$ and *WT*. ANOVA was used to determine whether there was a statistical significance of bouton turnover across times and genotypes.

ACKNOWLEDGMENTS. This work was supported by NIH Grant NS089683.

1. Marik SA, Yamahachi H, McManus JN, Szabo G, Gilbert CD (2010) Axonal dynamics of excitatory and inhibitory neurons in somatosensory cortex. *PLoS Biol* 8(6): e1000395.
2. Marik SA, Yamahachi H, Meyer zum Alten Borgloh S, Gilbert CD (2014) Large-scale axonal reorganization of inhibitory neurons following retinal lesions. *J Neurosci* 34(5): 1625–1632.
3. Yamahachi H, Marik SA, McManus JN, Denk W, Gilbert CD (2009) Rapid axonal sprouting and pruning accompany functional reorganization in primary visual cortex. *Neuron* 64(5):719–729.
4. Gilbert CD, Wiesel TN (1992) Receptive field dynamics in adult primary visual cortex. *Nature* 356(6365):150–152.
5. Abe H, et al. (2015) Adult cortical plasticity studied with chronically implanted electrode arrays. *J Neurosci* 35(6):2778–2790.
6. Marik SA, Olsen O, Tessier-Lavigne M, Gilbert CD (2013) Death receptor 6 regulates adult experience-dependent cortical plasticity. *J Neurosci* 33(38):14998–15003.
7. Xu K, Olsen O, Tzvetkova-Robev D, Tessier-Lavigne M, Nikolov DB (2015) The crystal structure of DR6 in complex with the amyloid precursor protein provides insight into death receptor activation. *Genes Dev* 29(8):785–790.

8. Olsen O, et al. (2014) Genetic analysis reveals that amyloid precursor protein and death receptor 6 function in the same pathway to control axonal pruning independent of β-secretase. *J Neurosci* 34(19):6438–6447.
9. Nikolaev A, McLaughlin T, O'Leary DD, Tessier-Lavigne M (2009) APP binds DR6 to trigger axon pruning and neuron death via distinct caspases. *Nature* 457(7232): 981–989.
10. Simon DJ, et al. (2012) A caspase cascade regulating developmental axon degeneration. *J Neurosci* 32(49):17540–17553.
11. Müller UC, Zheng H (2012) Physiological functions of APP family proteins. *Cold Spring Harb Perspect Med* 2(2):a006288.
12. Hsieh H, et al. (2006) AMPAR removal underlies Abeta-induced synaptic depression and dendritic spine loss. *Neuron* 52(5):831–843.
13. Kim TW, et al. (1995) Selective localization of amyloid precursor-like protein 1 in the cerebral cortex postsynaptic density. *Brain Res Mol Brain Res* 32(1):36–44.
14. Lyckman AW, Confaloni AM, Thinakaran G, Sisodia SS, Moya KL (1998) Post-translational processing and turnover kinetics of presynaptically targeted amyloid precursor superfamily proteins in the central nervous system. *J Biol Chem* 273(18): 11100–11106.
15. Back S, et al. (2007) beta-amyloid precursor protein can be transported independent of any sorting signal to the axonal and dendritic compartment. *J Neurosci Res* 85(12): 2580–2590.
16. Hoe HS, et al. (2009) Interaction of reelin with amyloid precursor protein promotes neurite outgrowth. *J Neurosci* 29(23):7459–7473.
17. Wang Z, et al. (2009) Presynaptic and postsynaptic interaction of the amyloid precursor protein promotes peripheral and central synaptogenesis. *J Neurosci* 29(35): 10788–10801.
18. Wilhelm BG, et al. (2014) Composition of isolated synaptic boutons reveals the amounts of vesicle trafficking proteins. *Science* 344(6187):1023–1028.
19. Mileusnic R, Lancashire CL, Johnston AN, Rose SP (2000) APP is required during an early phase of memory formation. *Eur J Neurosci* 12(12):4487–4495.
20. Müller U, et al. (1994) Behavioral and anatomical deficits in mice homozygous for a modified beta-amyloid precursor protein gene. *Cell* 79(5):755–765.
21. Phinney AL, et al. (1999) Cerebral amyloid induces aberrant axonal sprouting and ectopic terminal formation in amyloid precursor protein transgenic mice. *J Neurosci* 19(19):8552–8559.
22. Ring S, et al. (2007) The secreted beta-amyloid precursor protein ectodomain APPs alpha is sufficient to rescue the anatomical, behavioral, and electrophysiological abnormalities of APP-deficient mice. *J Neurosci* 27(29):7817–7826.
23. Lee KJ, et al. (2010) Beta amyloid-independent role of amyloid precursor protein in generation and maintenance of dendritic spines. *Neuroscience* 169(1):344–356.
24. Tyan SH, et al. (2012) Amyloid precursor protein (APP) regulates synaptic structure and function. *Mol Cell Neurosci* 51(1-2):43–52.
25. Weyer SW, et al. (2014) Comparative analysis of single and combined APP/APLP knockouts reveals reduced spine density in APP-KO mice that is prevented by APPsα expression. *Acta Neuropathol Commun* 2:36.
26. Seabrook GR, et al. (1999) Mechanisms contributing to the deficits in hippocampal synaptic plasticity in mice lacking amyloid precursor protein. *Neuropharmacology* 38(3):349–359.
27. Stahl R, et al. (2014) Shedding of APP limits its synaptogenic activity and cell adhesion properties. *Front Cell Neurosci* 8:410.
28. Obata S, Obata J, Das A, Gilbert CD (1999) Molecular correlates of topographic reorganization in primary visual cortex following retinal lesions. *Cereb Cortex* 9(3): 238–248.
29. Kallop DY, et al. (2014) A death receptor 6-amyloid precursor protein pathway regulates synapse density in the mature CNS but does not contribute to Alzheimer's disease-related pathophysiology in murine models. *J Neurosci* 34(19):6425–6437.
30. Small DH, et al. (1999) Neurite-outgrowth regulating functions of the amyloid protein precursor of Alzheimer's disease. *J Alzheimers Dis* 1(4-5):275–285.
31. Ando K, et al. (1999) Role of phosphorylation of Alzheimer's amyloid precursor protein during neuronal differentiation. *J Neurosci* 19(11):4421–4427.
32. Klevanski M, et al. (2015) The APP Intracellular Domain Is Required for Normal Synaptic Morphology, Synaptic Plasticity, and Hippocampus-Dependent Behavior. *J Neurosci* 35(49):16018–16033.